Determination of kinetic parameters of MgO-C

B. Hashemi, Z. Moghimi, Z.A. Nemati and S.K. Sadrnezhaad
Department of Materials Science and Engineering
Sharif University of Technology
Tehran, Iran, 11365-9466

ABSTRACT

Based on the kinetics relationships of a solid – gas model, a software was developed for the prediction of oxidation. Preliminary prediction of oxidation by the software and experimental results of MgO-C refractories were studied and compared. By using the obtained data from this approach, the effective diffusion coefficient, intermolecular diffusion coefficient and diffusion activation energy in the MgO-C refractories, containing various amount of graphite were obtained at different temperatures. First of all, the prediction by the software was very compatible with experimental results, for different oxidation mechanisms in the MgO-C refractories. The results showed that pore diffusion is the predominant oxidation mechanism in this system. The results indicated that when graphite content was above 10wt%, the intermolecular diffusion coefficient was independent from graphite content, and it was closed to a constant value at each temperature.

Advances in Refractories for the Metallurgical Industries IV
Fourth International Symposium
43 rd Annual Conference of Metallurgists of CIM
Hamilton. Ontario. Canada
Edited by M. Rigaud and C. Allaire

Introduction

The presence of graphite in MgO-C refractories causes high resistance to slag corrosion and thermal shock [1, 2]. But direct or indirect oxidation of graphite degrades these properties. Direct oxidation takes place due to gas-solid reactions and increases with temperature, while indirect oxidation is because of solid-solid reactions (reduction of MgO by graphite) at temperatures above 1400°C. Reduction of MgO results in the creation of Mg vapor and subsequence condensation of it at the surface of refractory produces dense layer of MgO. In other words, based on the scientific literatures both, direct and indirect oxidations are important in MgO-C refractories, but at different temperature ranges [3-5].

In steel making furnaces, oxidized atmosphere during lancing of oxygen, tapping or waiting time, causes graphite oxidation takes place and solid-gas reactions must be considered [6-8]. Different solid-gas models exist in the literature, but none of them has been used for oxidation kinetic determination of graphite in MgO-C refractories [9-11]. There are some studies regarding the oxidation studies, such as works that have been done by Li and Rigaud [12] according to gas analysis or Ghosh et al [13], Faghihi and Yamauchi [14] and Rongti et al, based on weight loss measurements in which they studied the oxidation kinetic of MgO-C refractories. But there is no general model for kinetic determination.

In this research, a computer software was developed by using a solid-gas model. Samples with different graphite content (4-18 wt %) were oxidized at different temperatures and fractional weight loss was measured and then it was compared with the prediction by the software. Oxidation mechanism and other information such as diffusion coefficient and activation energy were determined by software.

EXPERIMENTAL PROCEDURE

Cylindrical samples with 30 mm diameter and 25 mm height were made of Chinese sintered magnesia with a purity of 97% (Table 1) and natural Chinese graphite flakes with an ash content of 5wt%. Size distributions of magnesia grains are shown in Table 2.

Table 1 – Chemical analysis and density of Chinese sintered magnesia.

Composition	MgO	CaO	SiO_2	Al_2O_3	Fe_2O_3	L.O.I
Percent	97.1	1.26	0.56	0.09	0.89	0.01
Density (gr/cm^3)	3.51					

Table 2- Size distribution of MgO grains

Size (mm)	3-5	2-3	0.1-2	< 0.1
Percent	22.5	14.2	49.2	14.1

The samples contained 4-18 wt% graphite and 5wt% liquid phenolic resin (Novalac) as binder. The samples were prepared in one directional die at pressure of 120 MPa. The specimens were tempered at 240ºC for 18h and then were heated at 600ºC for 5 hr in a coke bed to remove the volatile species of resin.

The samples were oxidized isothermally at 1000ºC, 1175ºC and 1350ºC in a tubular furnace with 4.5 cm inside diameter and 45 cm height (as shown in Fig 1), under natural convection of air from bottom to top of the furnace. In other words, the air can flow easily through the tube. Each test sample was placed on an alumina tube that could be inserted, gradually, into the hot furnace at desired temperature in 2-3 min and then weight loss was recorded versus time. In order to have only the oxidation from side walls, the two ends of sample were covered by alumina plates. The fractional weight loss was calculated (X) according to:

$$Fractional \quad weight \quad loss = X = \frac{Weight \quad loss \quad at \quad time \quad t}{Total \quad weight \quad loss \quad after \quad complete \quad oxidation}$$

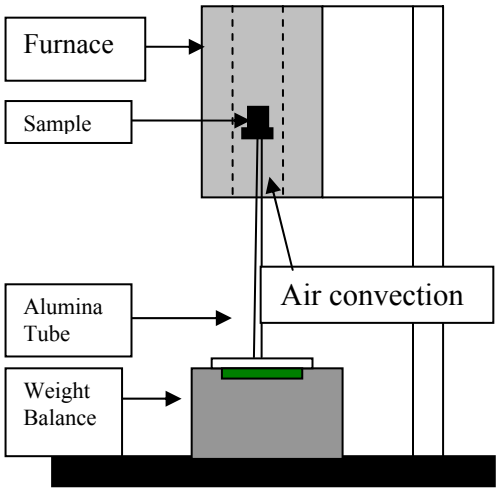

Fig. 1. Schematic view of setup used for weight loss measuring.

Modeling:

An isothermal solid-gas reaction model with constant dimension [9] was used. In this model (Fig. 2) three steps, mass transfer from gas layer or external diffusion, gas diffusion inward and outward through oxidized layer or pore diffusion and chemical reaction rate at reaction surface are being considered independently or in combination. As shown in Fig. 2 the unoxidized area is separated from the oxidized layer by a sharp boundary. Existence of a sharp boundary indicates that the reaction surface advances inwards the center of the sample. The total reaction time is related to the mentioned steps or mechanisms by equation (1) [9].

$$t = \tau_{che} \times f_{che}(x) + \tau_{dif} \times f_{dif}(x) + \tau_{ext} \times f_{ext}(x) \qquad (1)$$

Where τ is total conversion time for each corresponding mechanism, x is fraction of weight loss and each function is defined as following:

$$f_{ext}(x) = x \therefore f_{che}(x) = 1 - \sqrt{(1-x)} \therefore f_{dif}(x) = x + (1-x) \times ln(1-x)$$

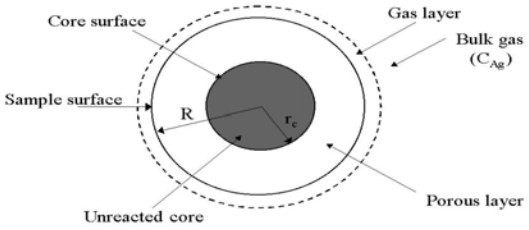

Fig. 2. Cross section of a cylindrical sample after reaction with gas.

The main parameter in this model, is the radius of unreacted core or r_c which is related to the fractional weight loss(x) by $X=1-(r_c/R)^2$ (where R is radius of sample). Equation (1) is the summation of three terms and for determination of the most important of them, the f(x) of each term is drawn versus time based on experimental data and best fit method. Slope of these lines indicate total conversion time (τ) of mechanisms and each line with minimum standard deviation represents the important mechanism or term. In this case a good fitness exists between fractional weight loss versus time resulting from experimental data and calculated data ($t = \tau.f(x)$). Sometimes the minimum standard deviation obtains when combination of mechanisms is considered.

Model algorithm:

Total conversation time of mechanisms is effective on oxidation and if it is assumed that they are positive, they can be derived by linear best fit method. Both least min square method and least vertical distance method are used for calculation of linear fitting. When one mechanism is dominant, both methods are applicable, but least vertical method is more accurate especially while a few data is available. Analytical solution of least min square relations is easier than least vertical relations, therefore former is used when more than one mechanism are effective on oxidation.

Solution of modeling relations:

1- One mechanism system

In one mechanism systems, a linear relationship exists between mechanism function and reaction time ($t = \tau \times f(x)$, where, t is reaction time, τ is total conversion time and f(x) is function of fractional weight change (x); that is determined by mechanism of solid-gas reaction). Therefore experimental results (x_i-t_i) are translated to a f(x)-time diagram for different mechanisms and a best fit line is calculated for each set of points (depending on mechanism type). The line with minimum standard deviation from experimental results shows the dominant mechanism in the system and slope of the lines indicates the τ value.

In least vertical distance method, vertical distance of each point to the line of $t = \tau\ f(X)$, is calculated and summation of vertical distances is minimized with changing of τ. For example, vertical distance of point A (t_i, $f(X_i)$) from line of $t = \tau\ f(X)$ (Fig. 2) i.e. distance of point A to point B (t_B, $f(X_B)$) will be:

$$d^2 = (f(x_B) - f(x_i))^2 + (\tau \times f(x_B) - t_i)^2 \qquad (2)$$

Where $\tau = \dfrac{f(x_i) - f(x_B)}{t_B - t_i}$ and $f(x_B) = \dfrac{\tau \times t_i + f(x_i)}{1 + \tau^2}$

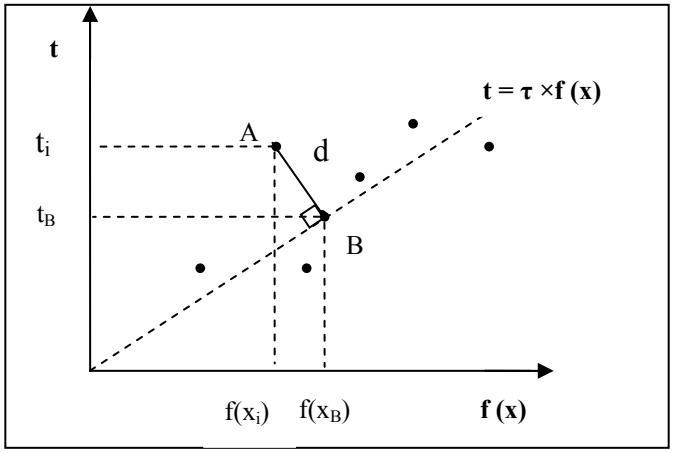

Fig. 2. Vertical distance of experimental results from line $t = \tau\ f(x)$

Therefore summation of vertical distances is:

$$\sum_{i=1}^{n} d_i^2 = \sum_{i=1}^{n} (f(x_B) - f(x_i))^2 + (\tau \times f(x_B) - t_i)^2 \qquad (3)$$

To minimize equation of (3),

$$\partial / \partial \tau \left(\sum_{i=1}^{n} (f(x_B) - f(x_i))^2 + (\tau \times f(x_B) - t_i)^2 \right) = 0 \qquad (4)$$

Eq.(4) has two roots only the positive root is acceptable.

$$\partial / \partial \tau \left(\sum_{i=1}^{n} \left(\frac{\tau \times t_i + f(x_i)}{1 + \tau^2} - f(x_i) \right)^2 + \left(\tau \times \frac{\tau \times t_i + f(x_i)}{1 + \tau^2} - t_i \right)^2 \right) = 0 \qquad (5)$$

$$\tau = \frac{\left(-\left(\sum_{i=1}^{n} (f(x_i)^2 - t_i^2)\right) + \sqrt{\left(\sum_{i=1}^{n} (f(x_i)^2 - t_i^2)\right)^2 + 4 \times \left(\sum_{i=1}^{n} (f(x_i) \times t_i)\right)^2}\right)}{4 \times \left(\sum_{i=1}^{n} (f(x_i) \times t)\right)}$$

2- Two mechanism systems:

In this system, deviation of experimental results from line $t = \tau_1 f_1(x) + \tau_2 f_2(x)$ were calculated by least min square method and summation of deviations was obtained by Eq. (6)

$$\sigma^2 = \sum_{i=1}^{n} [t_i - \tau_1 \times f_1(x_i) - \tau_2 \times f_2(x_i)]^2 \qquad (6)$$

Minimum summation of deviation derived when:

$$\frac{\partial \sigma^2}{\partial \tau_1} = 0 \qquad (7) \qquad\qquad \frac{\partial \sigma^2}{\partial \tau_2} = 0 \qquad (8)$$

Solution of Eqs. (7, 8) resulting to:

$$\tau_1 \times \sum_{i=1}^{n} f_1(x_i)^2 + \tau_2 \times \sum_{i=1}^{n} f_1(x_i) \times f_2(x_i) = \sum_{i=1}^{n} t_i \times f_1(x_i) \qquad (9)$$

$$\tau_1 \times \sum_{i=1}^{n} f_1(x_i) \times f_2(x_i) + \tau_2 \times \sum_{i=1}^{n} f_2(x_i)^2 = \sum_{i=1}^{n} t_i \times f_2(x_i) \qquad (10)$$

With substitution of each mechanism function instead of f_1 and f_2 , τ values are calculated.

3- Three mechanisms systems

In this system such as two mechanism systems, least min square method was used for determination of deviations result in:

$$\sigma^2 = \sum_{i=1}^{n} (t_i - \tau_{che}\, f_{che}(x_i) - \tau_{dif}\, f_{dif}(x_i) - \tau_{ext}\, f_{ext}(x_i))^2 \qquad (11)$$

To minimize deviation, derivation of Eq. (11) with respect to $\boldsymbol{\tau_1}$, $\boldsymbol{\tau_2}$ and $\boldsymbol{\tau_3}$ must be zero that is:

$$\frac{\partial \sigma^2}{\partial \tau_1} = 0 \quad , \quad \frac{\partial \sigma^2}{\partial \tau_2} = 0 \quad , \quad \frac{\partial \sigma^2}{\partial \tau_3} = 0$$

$$\tau_{che} \times \sum_{i=1}^{n} f_{che}(x_i)^2 + \tau_{dif} \times \sum_{i=1}^{n} f_{che}(x_i) \times f_{dif}(x_i) + \tau_{ext} \times \sum_{i=1}^{n} f_{che}(x_i) \times f_{ext}(x_i) = \sum_{i=1}^{n} t_i \times f_{che}(x_i)$$

$$\tau_{che} \times \sum_{i=1}^{n} f_{che}(x_i) \times f_{dif}(x_i) + \tau_{dif} \times \sum_{i=1}^{n} f_{dif}(x_i)^2 + \tau_{ext} \times \sum_{i=1}^{n} f_{dif}(x_i) \times f_{ext}(x_i) = \sum_{i=1}^{n} t_i \times f_{dif}(x_i)$$

$$\tau_{che} \times \sum_{i=1}^{n} f_{che}(x_i) \times f_{ext}(x_i) + \tau_{dif} \times \sum_{i=1}^{n} f_{dif}(x_i) \times f_{ext}(x_i) + \tau_{ext} \times \sum_{i=1}^{n} f_{ext}(x_i)^2 = \sum_{i=1}^{n} t_i \times f_{ext}(x_i)$$

By solving the above equation systems, τ values were obtained.

Results and discussion

Standard deviation of experimental results from best fit lines which have been used in calculation of total conversion time of different mechanisms were presented in Table 3. As mentioned before the best fit between oxidation and software results were obtained when deviation value were near to zero. In one mechanism condition; minimum standard deviation values were related to the pore diffusion mechanism. Oxidation and software results of samples containing 13 wt%G at 1000, 1175 and 1350°C were shown in Figs.3-5; based on fractional weight loss versus time. The figures indicate that, the pore diffusion is the main mechanism in oxidation of MgO-C samples. But no complete fitness of experimental results was obtained to calculated diffusion results. This indicates that other mechanism may be effective on the oxidation. So that the lowest standard deviations were obtained in two mechanisms condition when diffusion was considered with external mechanism. The best fitting between experimental results and two mechanisms software results was shown in Fig. 6.

Table 3- Standard deviation of oxidation results from best fit line for different mechanisms

Sample	Graphite %	Temperature °C	Mechanism Deviations				
			Chemical	Diffusion	External	Diff&Ext	Diff&Che
4g1	4.5	1350	13.91	1.43	23.45	1.13	1.12
4g2	4.5	1175	14.88	3.35	25.4	2.27	2.44
4g3	4.5	1000	18.0	1.98	22.93	….	…..
9g1	9	1350	13.7	6.68	27.83	1.57	2.19
9g2	9	1175	16.7	5.96	26.15	2.05	2.21
9g3	9	1000	21.17	2.07	28.53	1.31	1.33
13g1	13	1350	14.4	5.38	25.04	1.48	1.74
13g2	13	1175	8.92	2.06	10.7	1.03	1.04
13g3	13	1000	15.7	3.26	20.44	.73	.72
17g1	17	1350	16	6.31	34.71	1.01	1.91
17g2	17	1175	23.1	7.56	37.48	1.46	1.6
17g3	17	1000	16.82	3.5	21.91	1.35	1.33

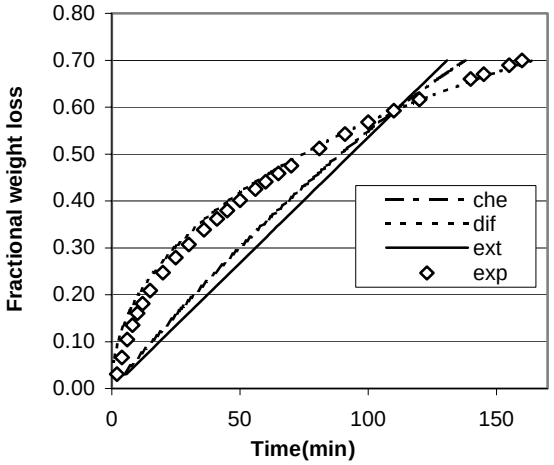

Fig. 3. Fractional weight loss of sample containing 13%G at 1000°C resulting from experimental and soft ware results

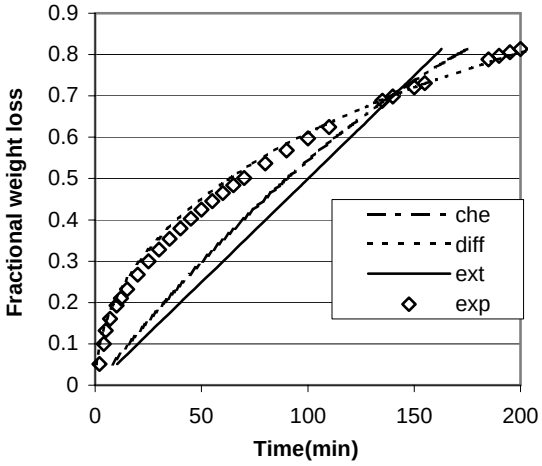

Fig. 4. Fractional weight loss of sample containing 13%G at 1175°C resulting from experimental and soft ware results

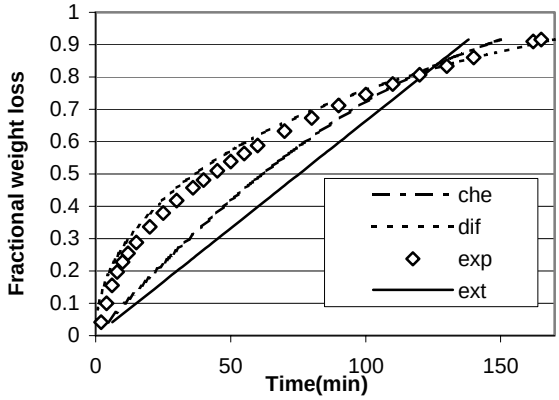

Fig. 5. Fractional weight loss of sample containing13%G at 1350°C resulting from experimental and soft ware results

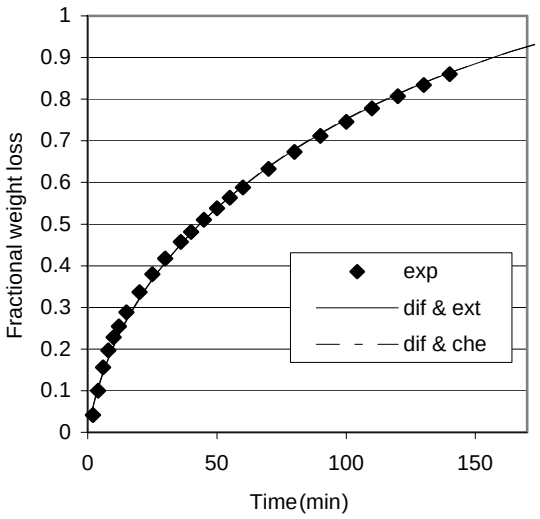

Fig 6 - Fractional weight loss of sample containing 13%G at 1350°C resulting from experimental and soft ware results at two mechanism system.

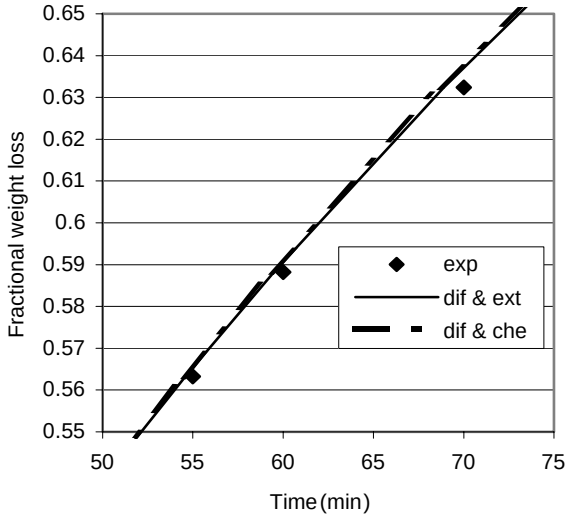

Fig 6.1- Enlarged part of fig 6

In Table 4; the diffusion total conversion time (τ_{dif}) of different samples were shown. They were calculated based on two mechanisms system results and then the effective diffusion coefficient (D_e) of samples were extracted through relation of them with D_e i.e.

$$\tau_{dif} = (\rho_m R^2)/(8C_{O2}D_e) \qquad (12)$$

Where ρ_m is molar density of graphite in samples, R is sample radius, C_{O2} is concentration of oxygen at the surface of samples in the system and D_e is effective diffusion coefficient. The effective diffusion coefficient of samples which increase with graphite content is shown in Fig.7. With increasing of graphite content of samples; higher porosity was produced in oxidized layer and then diffusivity of O_2 and CO was increased in oxidized layer.

Table 4. Diffusion total conversion time, initial porosity and graphite molar density of samples.

Sample	Temperature °C	Molar density of graphite	τ_{diff} min	Porosity %
4G1	1350	0.0108	167.2	13.5
4G2	1175	0.0108	200.4	13.6
4G3	1000	0.0108	328.4	13.4
9G1	1350	0.0207	182.3	11.9
9G2	1175	0.0207	265.7	11.9
9G3	1000	0.0207	396.1	11.8
9G4	900	0.0206	461.7	12.0
13G1	1350	0.0293	198.8	11.5
13G2	1175	0.0295	287.2	11.4
13G3	1000	0.0294	420	11.4
17G1	1350	0.0371	213	11.3
17G2	1175	0.0372	304.1	11.5
17G3	1000	0.0371	433	11.3

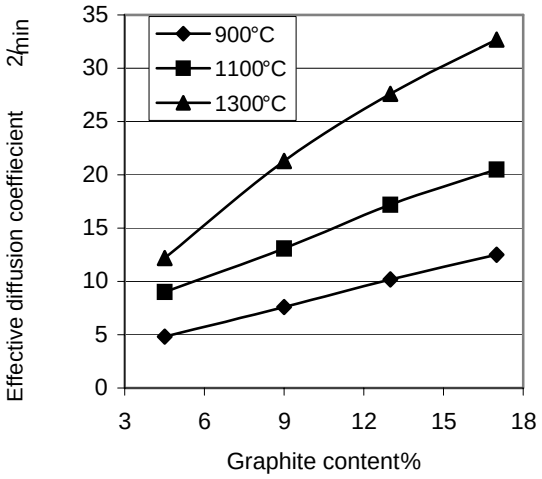

Fig. 7. Effective diffusion coefficient versus graphite content

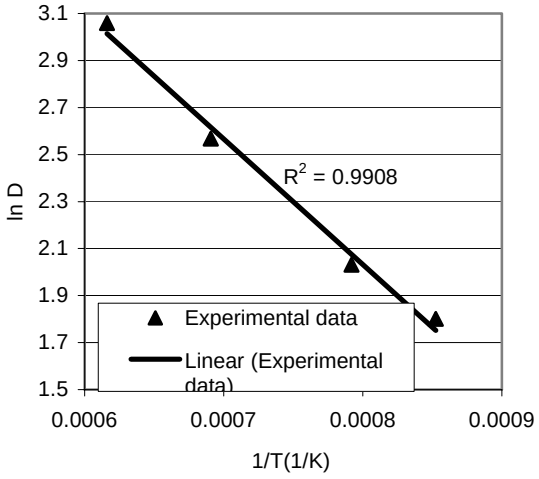

Fig. 8. Variation of $Ln(D_e)$ versus temperature of samples containing 9 wt% G

In Fig. 8; variation of effective diffusion coefficient of samples containing 9 wt%G versus temperature is shown. Linear relation of $\ln(D_e)$ with (1/T) is due to exponential relation of them and slope of line represents the activation energy of diffusion. The average of diffusion activation energy of samples was about 46.4±2 (KJ/mole).

Diffusion inward of air and outward of CO through porous oxidized layer takes place by one or combination of three mechanisms, molecular diffusion, Knudsen diffusion and surface diffusion based on pore structure and pore volume of oxidized layer of samples. In such a case, the effective diffusion coefficient is defined as [10]:

$$D_e = D_{O_2-CO}\frac{\varepsilon}{\tau} \quad \textbf{(12)}$$

(Where $\mathbf{D_{O2\text{-}CO}}$ is the molecular diffusivity of oxygen in CO, $\boldsymbol{\varepsilon}$ is the total porosity content of oxidized layer and $\boldsymbol{\tau}$ is the tortuosity of pore structure. Since determination of $\boldsymbol{\tau}$ is difficult it is approximated by the term $\varepsilon^{-1/2}$ [10]). The total porosity content of oxidized layer was calculated based on initial porosity and graphite volume percent of samples. According to equation 12 and ε value of samples, $D_{O2\text{-}CO}$ was derived and Fig. 9 shows the variation of $D_{O2\text{-}CO}$ versus graphite content of samples. The value of $D_{O2\text{-}CO}$ is nearly a constant value at each temperature when the graphite or porosity content of oxidized layer increases and it is independent of the porosity content of oxidized layer. According to Szekely et al. [16], it indicates that the molecular diffusion is predominant at high graphite content and the gaseous diffusivity through the porous layer is independent of the pore size. Value of intermolecular diffusion coefficient at samples contain 4.5 wt% graphite may be due to lower total porosity of samples and deviation of diffusion mechanism from pure molecular diffusion mechanism to a mixed mechanism.

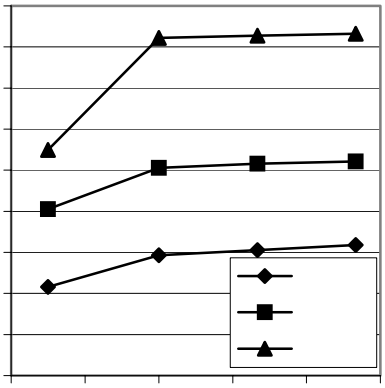

Fig. 9. Inter molecular diffusion coefficient versus graphite content

Conclusion

1- The Software was a suitable program in extraction of kinetic data.

2- According to oxidation condition, calculated effective diffusion coefficient can be used for estimation of oxidation time.

3- Molecular diffusion was predominant mechanism in oxidation of high graphite content samples.

References

1. Yamaguchi, S. Zhang and S. Hashimoto, Behavior of antioxidants added to carbon-containing refractories, Unitecr Proceedings 95, 1995, pp. 341-348.
2. S. Banerjee, Recent developments in steel – making refractories, Unitecr'01 Proceedings, pp.1033-1041, 2001.
3. Watanabe, H. Takahashi and F. Nakatani, Mechanism of dense magnesia layer formation near the surface of magnesia-carbon brick, J. Am. Ceram. Soc., 69[9] c-213-c-214 (1986).
4. Baker and B. Brezny, Dense zone formation in magnesia-graphite refractories, Unitecr Proceedings 91, pp. 168-172, 1991.
5. Yamaguchi, Control of oxidation-redaction in MgO-C refractories, Taikabutsu overseas, Vol.4, No.1, pp.32-37, 1984. –
6. M. Rigaud, C. Richmond and P. Bombard, Oxidation kinetics of graphite in basic refractory composites, Unitecr 91, p.266.
7. V.L. Lou, T.E. Mitchell and A.H. Heuer, Graphical displays of the thermodynamics of high-temperature gas-solid reactions and their application to oxidation of metals and evaporation of oxides, J. Am. Ceram. Soc., 68[2] 1985 49-58.
8. Yamaguchi, Affects of oxygen and nitrogen partial pressure on stability of metal, carbide, nitride and oxide in carbon-containing refractories, Taikabutsu overseas, Vol.7, No.1, pp.4-13, 1987.
9. N. Mazet and B. Spinner, Modeling of gas-solid reactions,
10. Missen, R. W. and Mims, C. A., Introduction to chemical reaction engineering and kinetics. John Wiley and Sons, Inc, New York, 1999, pp.224-236.

11. O. Levenspiel, Chemical reaction engineering, John Wiley & Sons, Inc. 1972, p.357.
12. Li, X., Rigaud, M. and Palco, S., Oxidation kinetics of graphite phase in magnesia-carbon refractories. J.Am.Ceram.Soc, 1995, **78**(4) 965-71.
13. Ghosh, N. K., Ghosh, D. N. and Jagannathan, K. P., Oxidation mechanism of MgO-C in air at various temperature. British Ceramic Transactions, 2000, **99**(3), pp.124-128.
14. Faghihi-Sani, M. A., and Yamaguchi, A., Oxidation kinetics of MgO-C refractory bricks, Ceramics International, 2002, 28, 835-839.
15. L. Rontgi, et. al, Kinetics of reduction of magnesia with carbon, Thermochimica Acta,390 (2002), 145-151.
16. J. Szekely, J.W. Evans and H.Y. Sohn, Gas-Solid Reactions , Academic press, New York, 1976, pp. 8-69.